ANTIMICROBIAL AGENTS AND CHEMOTHERAPY, Feb. 2011, p. 788–797 Vol. 55, No. 2
0066-4804/11/$12.00 doi:10.1128/AAC.01098-10

Interaction of W-Substituted Analogs of Cyclo-RRRWFW with Bacterial Lipopolysaccharides: the Role of the Aromatic Cluster in Antimicrobial Activity▽†

Mojtaba Bagheri,[1] Sandro Keller,[1,2] and Margitta Dathe[1]*

Leibniz Institute of Molecular Pharmacology (FMP), Robert-Rössle-Str. 10, 13125 Berlin,[1] and Molecular Biophysics, University of Kaiserslautern, Erwin-Schrödinger-Str. 13, 67663 Kaiserslautern,[2] Germany

Received 9 August 2010/Returned for modification 2 September 2010/Accepted 21 October 2010

The activity of cyclo-RRRWFW (c-WFW) against *Escherichia coli* has been shown to be modulated by the aromatic motif and the lipopolysaccharides (LPS) in the bacterial outer membrane. To identify interaction sites and to elucidate the mode of c-WFW action, peptides were synthesized by the replacement of tryptophan (W) with analogs having altered hydrophobicity, dipole and quadrupole moments, hydrogen-bonding ability, amphipathicity, and ring size. The peptide activity against *Bacillus subtilis* and erythrocytes increased with increasing hydrophobicity, whereas the effect on *E. coli* revealed a more complex pattern. Although they had no effect on the *E. coli* inner membrane even at concentrations higher than the MIC, peptides permeabilized the outer membrane according to their antimicrobial activity pattern, suggesting a major role of LPS in peptide transport across the wall. For isothermal titration calorimetry (ITC) studies of peptide-lipid bilayer interaction, we used POPC (1-palmitoyl-2-oleoyl-*sn*-glycero-3-phospho-choline), either alone or in mixtures with 1-palmitoyl-2-oleoyl-*sn*-glycero-3-[phospho-*rac*-(1-glycerol)] (POPG), to mimic the charge properties of eukaryotic and bacterial membranes, respectively, as well as in mixtures with lipid A, rough LPS, and smooth LPS as models of the outer membrane of *E. coli*. Peptide accumulation was determined by both electrostatic and hydrophobic interactions. The susceptibility of the lipid systems followed the order of POPC-smooth LPS >> POPC-rough LPS > POPC-lipid A = POPC-POPG > POPC. Low peptide hydrophobicity and enhanced flexibility reduced binding. The influence of the other properties on the free energy of partitioning was low, but an enhanced hydrogen-bonding ability and dipole moment resulted in remarkable variations in the contribution of enthalpy and entropy. In the presence of rough and smooth LPS, the binding-modulating role of these parameters decreased. The highly differentiated activity pattern against *E. coli* was poorly reflected in peptide binding to LPS-containing membranes. However, stronger partitioning into POPC-smooth LPS than into POPC-rough LPS uncovered a significant role of O-antigen and outer core oligosaccharides in peptide transport and the permeabilization of the outer membrane and the anti-*E. coli* activity of the cyclic peptides.

Cationic antimicrobial peptides (CAPs) are key components of the innate immune systems of virtually all organisms (52). Because of their toxicity against a broad variety of bacterial species and their nonspecific membrane-disturbing mode of action, they are regarded as promising peptide-based therapeutics. Parameters such as conformation, charge, hydrophobicity, and amphipathicity have been identified as the main factors that modulate membrane binding and influence bacterial selectivity (16).

In contrast to linear, helix-forming CAPs, the structural determinants and modes of interaction of short and conformationally constrained peptides with cellular membranes are less understood (26). Among these peptides are sequences rich in particular amino acids such as W and arginine (R) (22, 24, 45). Recently, it has been shown that the head-to-tail cyclization of the synthetic hexapeptide acetyl (Ac)-RRWWRF-NH_2 (Ac-RW) identified by the screening of synthetic combinatorial libraries (12) distinctly enhances the activity against Gram-negative *Escherichia coli* (14). However, in contrast to its high antimicrobial activity, the cyclic peptide permeabilizes lipid bilayers only weakly. Single-amino-acid substitutions or the replacement of L-amino acid residues by D-enantiomers enhance or abolish the antimicrobial activity (14, 39, 50). Cyclo-RRWWRF (c-RW) and related analogs are able to permeabilize the outer and inner membranes of *E. coli* (29), but, interestingly, the activity decreases against outer wall-deficient L forms of *E. coli*. Moreover, studies with mutant *E. coli* strains demonstrated that the activity of sequences with three adjacent aromatic residues, for instance, cyclo-RRRWFW (c-WFW), is reduced upon the removal of the O-antigen and the shortening of the core region of the outer membrane LPS (29). This points to a particular role of LPS in peptide activity and selectivity against *E. coli* membranes.

In interaction with detergents and lipids, c-RW and c-WFW develop pronounced amphipathicity (5, 6). The peptide backbone lies parallel to the lipid bilayer surface, the positively charged R residues interact with the phosphate groups of the lipids, and aromatic residues insert into the membrane (7). Lipid demixing and domain formation in 1,2-dipalmitoyl-*sn*-glycero-3-[phospho-*rac*-(1-glycerol)]–1,2-dipalmitoyl-*sn*-glycero-3-phosphoethanolamine bilayers have

* Corresponding author. Mailing address: Leibniz Institute of Molecular Pharmacology (FMP), Robert-Rössle-Str. 10, 13125 Berlin, Germany. Phone: 49 30 94793274. Fax: 49 30 94793159. E-mail: dathe@fmp-berlin.de.

† Supplemental material for this article may be found at http://aac.asm.org/.

▽ Published ahead of print on 22 November 2010.

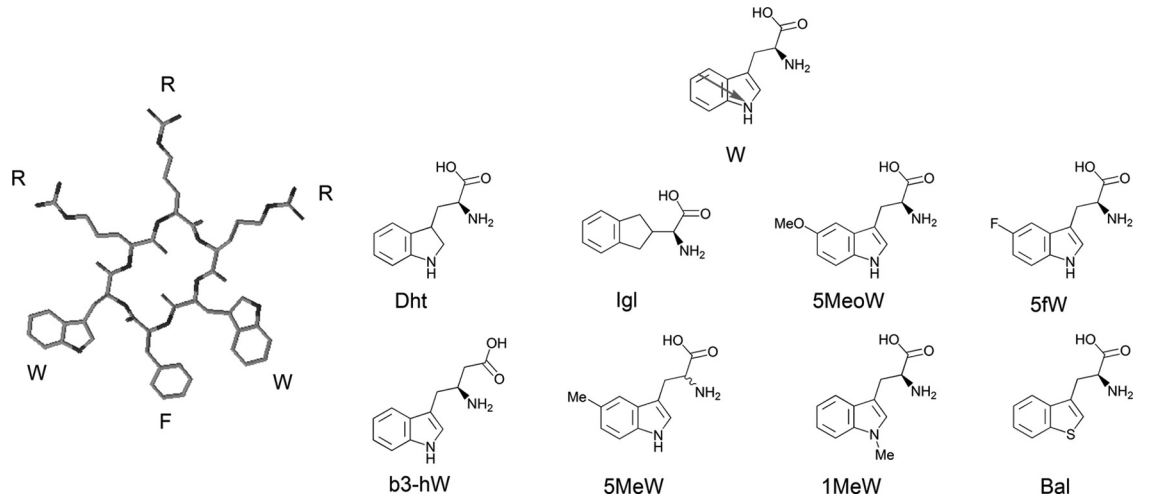

FIG. 1. Structures of c-WFW (left) and W analogues (right) used in this study. The structure of the parent peptide is based on the previously published nuclear magnetic resonance study (6). The arrow shows the dipole moment of W residue (~2.1 D), which is directed from C-5 in the six-membered ring of the indole moiety to N-1 in the five-membered ring.

been suggested as the basis for the selective antibacterial action of c-RW (8).

The observation that many cyclic hexapeptides are similar in conformation but differ in sequence (5) and antimicrobial activity raises the question of whether specific amino acid residues are responsible for the activity and selectivity of the RW-rich sequences against Gram-negative bacteria. Studies using trimesic acid as a template mimicking the peptide backbone (4) demonstrated an essential role of the guanidino moiety for bacterial selectivity. However, it seems that not only charge-driven peptide accumulation at negatively charged *E. coli* membranes but also the exact nature of the interaction of W residues with LPS domains is important.

To investigate the role of the aromatic motif in c-WFW in interaction with bacterial membranes, we synthesized a set of cyclic hexapeptide analogs carrying replacements of W residues by unnatural residues. The substituents differ in terms of hydrophobicity, dipole and quadrupole moments, ability to form hydrogen bonds, and amphipathicity from W. They include dihydrotryptophan (Dht), α-(2-indanyl)glycine (Igl), 5-methoxy-L-tryptophan (5MeoW), 5-fluoro-L-tryptophan (5fW), 5-methyl-DL-tryptophan (5MeW), 1-methyl-L-tryptophan (1MeW), and β-(benzothien-3-yl)-alanine (Bal) (Fig. 1 and Table 1). In addition, the β-amino acid L-β-homotryptophan (b3-hW) was introduced to increase the size of the backbone ring. The activities of the peptides were evaluated against Gram-negative *E. coli* (strain DH5α) and Gram-positive *Bacillus subtilis* (strain DSM 347) bacteria and human red blood cells (RBCs). Also, the permeabilization of outer and inner membranes determined using *E. coli* (strain ML-35p) provided evidence for the mode of action of the peptides and their ability to reach the cytoplasmic membrane, which is considered to be the target of most CAPs (36). To correlate the activity profiles with the driving forces of peptide-membrane interaction, peptide binding to different membrane model systems was studied by way of isothermal titration calorimetry (ITC) (48). Binding parameters were derived by applying a surface partition equilibrium model combined with

TABLE 1. List of peptides, amino acid sequences, RP-HPLC retention times (t_R), antimicrobial activities, and hemolytic activities

Peptide	Amino acid sequence	t_R[a] (min)	Peptide MIC[b] (μM) against:		Hemolysis[c] (%)
			B. subtilis (DSM 347)	*E. coli* (DH 5α)	
c-(Dht)F(Dht)[d]	c-RRR(Dht)F(Dht)	9.92	50	200	1
c-(Igl)F(Igl)[d]	c-RRR(Igl)F(Igl)	15.91	25	200	3
c-WFW	c-RRRWFW	18.83	3.1	3.1	6
c-(5MeoW)F(5MeoW)	c-RRR(5MeoW)F(5MeoW)	19.08	3.1	12.5	1
c-(5fW)F(5fW)	c-RRR(5fW)F(5fW)	19.92	1.6	3.1	ND[e]
c-(b3-hW)F(b3-hW)	c-RRR(b3-hW)F(b3-hW)	20.06	6.3	50	1
c-(5MeW)F(5MeW)[d]	c-RRR(5MeW)F(5MeW)	20.37	3.1	6.3	5
c-(1MeW)F(1MeW)	c-RRR(1MeW)F(1MeW)	20.41	3.1	6.3	27
c-(Bal)F(Bal)	c-RRR(Bal)F(Bal)	22.03	1.6	12.5	70
Ac-WFW	Ac-RRWFWR-NH_2	16.58	50	400	ND[e]

[a] t_R is the RP-HPLC retention time, a measure of peptide hydrophobicity and amphipathicity.
[b] Values represent the means from three independent experiments performed in triplicate. Standard deviations were <5%.
[c] Values represent the percentage of release of hemoglobin from human RBCs upon incubation with cyclic peptides at c_P = 200 μM.
[d] These unnatural amino acids are a mixture of at least two enantiomers.
[e] ND, not determined.

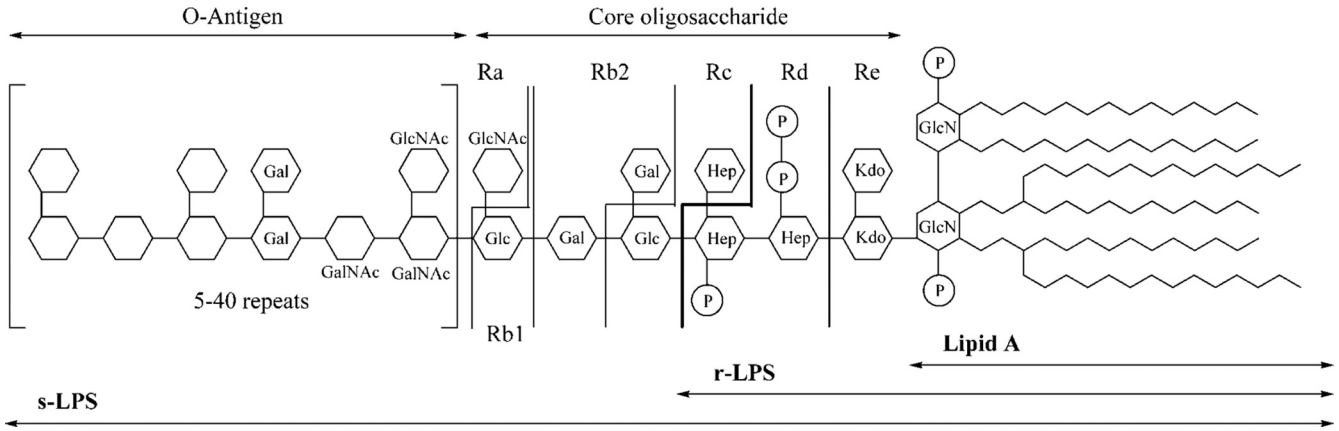

FIG. 2. General structure of *E. coli* LPS. The sugar moieties in the core region and the composition of lipid A are conserved in different *E. coli* strains. However, the O-antigen region varies strongly. Charged residues are located preferentially in the core oligosaccharide region. Ra to Re denote the different rough chemotypes of LPS. The rough-LPS (r-LPS) used in this study is of the Rd chemotype. Native, complete LPS is called smooth-LPS (s-LPS). Gal, galactose; GalNAc, *N*-acetyl-galactosamine; Glc, glucose; GlcN, glucosamine; GlcNAc, *N*-acetyl-glucosamine; Kdo, 2-keto-3-deoxyoctonic acid; Hep, L-glycerol-D-manno-heptose.

Gouy-Chapman theory to account for electrostatic effects at the membrane surface (30, 31, 43). The lipid bilayers used in this study were composed of 1-palmitoyl-2-oleoyl-*sn*-glycero-3-phospho-choline (POPC), either alone or in mixture with 1-palmitoyl-2-oleoyl-*sn*-glycero-3-[phospho-*rac*-(1-glycerol)] (POPG) (3:1 [mol/mol]) to model the electrostatic properties of erythrocyte and bacterial target membranes, respectively. POPC bilayers doped with diphosphoryl lipid A (LA), rough LPS (r-LPS or Rd-LPS), and smooth LPS (s-LPS) (Fig. 2) were used to assess the contribution of outer membrane LPS components to peptide activity against *E. coli*.

MATERIALS AND METHODS

Compounds. 9-Fluorenylmethoxycarbonyl (Fmoc)-N-protected amino acids were obtained from GL Biochem, Ltd., China. Fmoc-dihydro-L-Trp(*t*-Boc)-OH and Fmoc-α-(2-indanyl)glycine-OH (both from Advanced ChemTech/ThuraMed), Fmoc-3-(3-benzothienyl)-L-alanine and Fmoc-L-β-homotrp-OH (both from Sigma-Aldrich, Germany), Fmoc-5-methyl-DL-Trp-OH and Fmoc-5-methoxy-L-Trp-OH (both from AnaSpec), Fmoc-1-methyl-L-Trp-OH (Bachem, Switzerland), and Fmoc-5-fluoro-L-Trp-OH (Iris Biotech, Germany) were obtained from the noted provider. All other chemicals and solvents were from Sigma-Aldrich or Fluka. Ampicillin, 2-nitrophenyl-β-D-galactopyranoside (ONPG), polymyxin sulfate (PMXB), Luria broth (LB), s-LPS from *E. coli* K-235, Rd-LPS from *E. coli* F583, and diphosphoryl LA from *E. coli* F583 (Rd mutant) were obtained from Sigma-Aldrich. Nitrocefin (NCF) was provided from by Oxoid, United Kingdom. POPC and POPG were purchased from Avanti Polar Lipids. Other chemicals used in biophysical experiments were from Merck, Germany.

Synthesis of cyclic peptides. Cyclic peptides were synthesized manually by solid-phase peptide synthesis (SPPS) using the standard Fmoc/*tert*-butyl (*t*-Bu) protocol as described in detail elsewhere (9). The peptides were purified by reversed-phase high-performance liquid chromatography (RP-HPLC) using a Shimadzu (Japan) LC-10A system operating at 220 nm to give final products that were >95% pure. Peptides were further characterized by matrix-assisted laser desorption-ionization mass spectrometry (MALDI-MS) (MALDI II; Kratos, United Kingdom) to confirm the correct molar masses. The calculated and observed molecular masses (in Da) of the peptides were found to be identical (data not shown). c-(5MeoW)F(5MeoW), c-(5fW)F(5fW), and c-(1MeW)F(1MeW) were provided by Biosyntan (Germany).

Analytical HPLC. Chromatographic characterization was performed on a Jasco (Japan) HPLC system using a diode array detector operating at 220 nm. Runs were carried out on a PolyEncap A 300 column (250 by 4.0 mm; Bischoff Analysentechnik, Germany). The sample concentration was 1 mg of peptide/ml in eluent A. The mobile phase A was 0.1% trifluoroacetic acid (TFA) in water, and phase B was 0.1% TFA in 80% acetonitrile-20% water (vol/vol). The retention time (t_R) of the peptides was determined using a linear gradient of 5 to 95% phase B during 40 min at room temperature.

Circular dichroism (CD) spectroscopy. Stock solutions of cyclic and linear peptides (2.5 mM) were prepared with buffer (10 mM phosphate buffer, 154 mM NaF, pH 7.4). An aliquot of this solution was diluted with either phosphate buffer or a 20 mM suspension of POPG small unilamellar vesicles (SUVs) in the same buffer to achieve the desired peptide (100 μM) and lipid (10 mM) concentrations. Measurements were carried out on a Jasco J-720 spectrometer (Japan) at 20°C. Thirty-five scans were accumulated. Peptide spectra were corrected by subtracting spectra of the corresponding buffer or peptide-free lipid suspensions. The presented spectra give the mean residual molar ellipticity (Θ_{mr}) in the 190- to 260-nm region.

Antimicrobial activity. The antimicrobial activity of the peptides was tested against Gram-negative *E. coli* (strain DH 5α) (optical density at 600 nm [OD_{600}] of 1.0, which corresponds to 2.2×10^8 cells/ml) and Gram-positive *B. subtilis* (strain DSM 347) (OD_{600} of 1.0, which corresponds to 8.8×10^7 cells/ml) using a 96-well microtiter plate assay as previously described (10). Bacteria were grown in LB. The inoculum was prepared from mid-log-phase cultures (OD_{600} of 0.4 ± 0.1). Fifty-μl aliquots of peptide solutions of various concentrations were added to the microtiter plate and incubated with 150 μl of the bacterial suspension, so that the final number of cells per well was 1.6×10^6 (*E. coli*) and 8×10^5 (*B. subtilis*). Final peptide concentrations were tested in triplicate and ranged from 100 to 0.05 μM in 2-fold dilutions. The highest concentration of the least active peptide was 400 μM. Cultures without peptide were used as controls. After 17 h of incubation at 37°C, the absorbance was read at 600 nm (Safire microplate reader; Tecan, Germany). The MIC was determined as the lowest peptide concentration at which no change in absorbance (i.e., no bacterial growth) was observed.

Hemolytic activity. Hemolytic activity was determined using human RBCs (Charité-Universitätsmedizin, Germany) as described before (10). A 100-μl cell suspension (2.5×10^9 cells/ml in 10 mM Tris, 150 mM NaCl, pH 7.4), aliquots of a peptide stock solution and buffer were pipetted into Eppendorf tubes to give a final volume of 1 ml and the desired peptide concentration. The suspensions containing 2.5×10^8 cells were incubated for 30 min under gentle shaking in an Eppendorf thermomixer. After being cooled in ice-water and centrifuged at 2,000 × *g* at 4°C for 5 min, 200 μl of the supernatant was mixed with 2,300 μl of 0.5% NH_4OH, and the absorbance was determined at 540 nm (Lambda 9; Perkin-Elmer, Germany). Zero hemolysis (blank) and 100% hemolysis (control) were read with cell suspensions incubated in buffer and 0.5% NH_4OH, respectively.

Permeabilization of inner and outer membranes. The permeabilizing activities against inner and outer membranes were assessed using *E. coli* (strain ML-35p) in 96-well microtiter plates (29, 35). The cells express periplasmic β-lactamase. NCF, a substrate of β-lactamase, normally is excluded from *E. coli* by the outer LPS layer as the strain lacks lactose permease. ONPG is cleaved by β-galactosidase, which is localized within the cytoplasm. However, the substrate is blocked

from cell entry by the inner membrane, since the strain lacks *lac* permease. As a result of peptide-induced membrane permeabilization, NCF and ONPG enter the cell, and their metabolization can be followed by color change from yellow to red and colorless to yellow, respectively.

The bacterial culture was grown in LB medium containing 100 μg/ml ampicillin until an OD_{550} of 0.3 (an OD_{550} of 1.0 corresponds to 3.8×10^8 cells/ml). Cells were rinsed twice and resuspended in HEPES buffer to an OD_{550} of 0.3. To assay inner membrane permeabilization, 50 μl of ONPG stock solution (300 μg/ml) and, for monitoring the outer membrane (OM) permeabilization, 50 μl of NCF stock solution (60 μg/ml) were pipetted into microtiter wells containing 50 μl peptide solution. Finally, a 50-μl cell suspension (OD_{550} of 0.3) was added, resulting in a final peptide concentration close to the individual MICs. The inner and outer membrane permeabilization was monitored spectrophotometrically during a time period of up to about 1 h at wavelengths of 420 and 500 nm, respectively, using a Safire microplate reader. The wells with PMXB at a concentration of 5 μM and without peptide were used as positive and negative controls, respectively. PMXB is a cationic, cyclic, acetylated decapeptide with high outer membrane-permeabilizing activity. Its activity is related to the rapid competitive displacement of divalent cations from the negative charges of LPS, followed by insertion into the hydrophobic fatty acid chain region (29, 35). The OM permeabilization rate ($\Delta OD/\Delta t$) of the peptides was derived as the change in the OD_{500} during the first 6.2 min.

Vesicle preparation. POPC and mixed POPC-POPG (3:1 [mol/mol]) lipid films were made as described previously (15). For the preparation of POPC-LA lipid films, dried LA (molar mass, 1,792 g/mol) was dissolved in chloroform-MeOH (2:1, vol/vol) to give a concentration of 2.5 mg/ml. A defined volume was added into a 10-ml round-bottomed glass tube prefilled with dried POPC to reach the desired molar ratio of POPC-LA (12:1 [mol/mol]). Solvent removal in a rotary evaporator followed by high-vacuum drying overnight provided a dry lipid film. Each LA molecule has two divalent phosphate anions ($[-OPO_3]^{-2}$), and thus the ratio of negative charges in POPC-LA (12:1 [mol/mol]) vesicles is identical to that in POPC-POPG (3:1 [mol/mol]).

For the preparation of LPS-containing vesicles, the well-characterized POPC was used as a matrix. We employed a protocol called the dry method for film preparation (18). The dried POPC-LPS (molar ratio, 12:1) lipid films were suspended in pyrogen-free water (Milli-Q; Element System; Millipore, France), extensively vortexed, and heated up to 60°C, followed by sonication in a bath sonicator for 10 min. After the suspension was vortexed, the cycle was repeated twice. The resulting turbid mixture was lyophilized. This protocol leads to the incorporation of a large amount of LPS into the POPC membrane (11). To prevent any contamination of the POPC-LPS preparation, no further attempt was made to separate nonincorporated LPS. Based on the structure of LPS shown in Fig. 2, we assumed that Rd-LPS from *E. coli* F583 (r-LPS) and s-LPS from *E. coli* K-235 have molar masses of ~2.5 and ~ 10 kg/mol, respectively. The assumed masses fit well with molar masses reported for the corresponding r-LPS and s-LPS of other Gram-negative strains (13, 38, 40).

As all negatively charged mono-($[-OPO_3-]^-$) and divalent phosphate anions and carboxylate groups ($[-CO_2]^-$) are located in the inner-core oligosaccharides of LPS, there is no difference in the negative charge between r-LPS and s-LPS. In this study, we considered the total negative charges of the phosphate anions (nine charges per molecule).

To prepare SUVs, dried lipid films were hydrated in pyrogen-free phosphate buffer (10 mM NaH_2PO_4-Na_2HPO_4, 154 mM NaF, pH 7.4). Final lipid concentrations were 40 mM for POPC, 20 mM for mixtures of POPC with POPG or LA, and 5 mM for mixtures of POPC and r-LPS or s-LPS. The suspensions were vortexed for 5 min and sonicated in an ice-water bath using an ultrasonicator (Sonopuls HD 2070; Bandelin Electronic, Germany) for 20 min (15). The mean diameter of SUVs was about 30 nm, as determined by dynamic light scattering on an N4 Plus particle sizer (Beckman Coulter).

ITC. High-sensitivity ITC was performed on a VP-ITC (GE Healthcare, Sweden). All experiments were run at 37°C to study peptide binding to POPC doped with LA and LPSs above the gel-to-liquid–crystalline-phase transition temperature. To determine lipid-peptide interactions, a 40 μM peptide solution in the calorimeter cell was titrated with an SUV suspension of 5 to 40 mM lipid concentration. All peptide solutions were degassed. In a typical experiment, 3- to 10-μl aliquots of the SUV suspension were titrated into a 40 μM peptide solution, and the content of the sample cell was stirred continuously at 310 rpm. Because of a small loss of titrant during the mounting of the syringe and the equilibration stage preceding the actual titration, we usually set the first injection volume to 3 to 5 μl and excluded the first peak from data analysis. Time spacings of 5 min were long enough to allow the ITC signal to return to the baseline value. The measured heat of binding decreased with consecutive lipid injections because less free peptide was available. Control experiments injecting lipid vesicles into buffer without peptide showed that the heats of dilution were small and constant. Baseline correction and peak integration were done as described by the manufacturer. Nonlinear least-squares data fitting was performed in an Excel (Microsoft) spreadsheet using the Solver add-in (Frontline Systems) (32).

RESULTS

Physicochemical properties of W analogs and peptide characterization. The peptide sequences used in this study (Table 1) are based on the previously described cyclic hexapeptide c-WFW, which contains three adjacent charged and three adjacent aromatic residues (50). In the presented analogs, we preserved key features such as the number and distribution of the three R and noncharged residues. The aromatic side chain of W is hydrophobic (17) and able to form hydrogen bonds, and it has a dipole moment of ~2.1 D (37). The hydrophobicity and amphipathicity of c-WFW are reflected in an HPLC retention time of 18.83 min (Table 1). Unnatural residues Dht, Igl, 5MeoW, 5fW, b3-hW, 5MeW, 1MeW, and Bal instead of W (Fig. 1, Table 1) alter the hydrophobicity, electron distribution, hydrogen-bonding ability, amphipathicity, and flexibility in the aromatic cluster of the peptide (see Table S1 in the supplemental material). The changed electron distribution of Dht conserves the hydrogen-bonding ability but reduces both the aromaticity and the dipole moment. Because of the protonation of the free electron pair of −NH− at physiological pH, c-(Dht)W(Dht) is much more hydrophilic (t_R = 9.92 min) than c-WFW (Table 1). Like W, Igl bears a fused-ring aromatic side chain that is, however, closer to the backbone. c-(Igl)F(Igl) is more hydrophilic than the parent peptide and is incapable of hydrogen bonding (Table 1). The introduction of 5MeoW, 5fW, 5MeW, or 1MeW only slightly enhances hydrophobicity compared to that of the parent peptide (19.08 min $< t_R <$ 20.41 min) (Table 1). The quadrupole and dipole moments of 5MeW and 1MeW (~2.2 D) are similar to those of W in magnitude and direction (37, 42). In contrast, a methoxy group (in 5MeoW) or fluorine atom (in 5fW) draws electrons to C-5 and enhances the dipole moment of the indole moiety. However, the density of negative charges above and below the plane of the indole ring is lower in the case of 5fW, which decreases the quadrupole moment compared to that of W (42). On the other hand, the methoxy group pushes electrons into the indole ring plane, thus strengthening the π-electron system and the quadrupole moment (42). The replacement of the hydrogen at C-5 by a methoxy group or fluorine atom also enhances the hydrogen-bonding character of the −NH− moiety, which is lost in 1MeW. The Bal-containing peptide is the most hydrophobic one in this series (t_R = 22.03 min). Because of the lower electronegativity of the sulfur atom, the dipole moment of Bal is lower than that of W. The side chain has no appreciable amphipathic structure and does not participate in hydrogen bonding (46). The incorporation of b3-hW enhances the size and flexibility of the backbone ring. Because of two extra methylene groups, c-(b3-hW)F(b3-hW) is slightly more hydrophobic than c-WFW (Table 1).

CD spectra of c-WFW, c-(b3-hW)F(b3-hW), and Ac-WFW. To obtain structural information on c-WFW, c-(b3-hW)F(b3-hW), and the linear Ac-WFW, we compared their conformations in buffer and the POPG-bound state with the aid of CD spectroscopy (Fig. 3). The spectra of c-WFW dissolved in

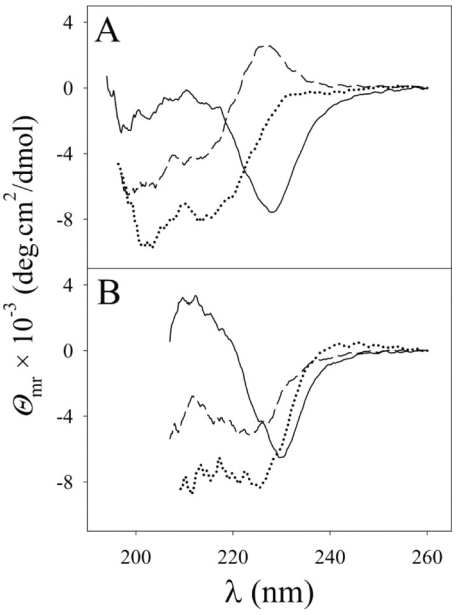

FIG. 3. CD spectra of c-(b3-hW)F(b3-hW) (solid line), c-WFW (dotted line), and Ac-WFW (dashed line) in phosphate buffer (A) and the presence of POPG SUVs (B).

buffer show negative bands at 200 and 220 nm. In contrast, Ac-WFW reveals a positive band at 225 nm and negative ellipticity values at low wavelengths (down to <200 nm), which is characteristic of small random-coil peptides (Fig. 3A). The binding of c-WFW to POPG SUVs results in only minor spectral changes, thus reflecting few conformational changes in the cyclic peptide (Fig. 3B). On the binding of Ac-WFW to POPG, the positive band at 225 nm disappears and the spectral characteristics become similar to those of c-WFW. As in the 225-nm region, the ellipticity contributions from the peptide bonds and the aromatic residues superimpose, changes in the Ac-WFW spectrum can be attributed to restrictions in the backbone structure and reorientation of the side chains (14) resulting in an amphipathic structure.

The b3-hW-containing peptide shows a sharp negative band at ~225 to 230 nm both in an aqueous environment and when bound to POPG membranes (Fig. 3). This points to a different orientation and environment of the aromatic residues compared to those of Ac-WFW and c-WFW. Additionally, the pronounced positive ellipticity of the POPG-bound peptide at lower wavelengths (210 nm), where the contribution of the backbone amide bonds predominates, suggests that binding reduces the number of backbone conformers. The CD signal could not be recorded reliably below 210 nm because of excessive light scattering by SUV suspensions in this wavelength range.

Antimicrobial and hemolytic activities. The antimicrobial activities of the cyclic peptides and Ac-WFW are summarized in Table 1. The cyclic peptides with t_R values between 18.83 and 22.03 min were highly active (1.6 μM < MIC < 6.3 μM) against *B. subtilis* with few differences. The slightly reduced activity of c-(b3-hW)F(b3-hW) compared to that of c-WFW correlates with an enhanced size and flexibility of the cyclic peptide backbone. In contrast, the hydrophilic c-(Dht)F(Dht) and c-(Igl)F(Igl) ($t_R \geq 15.9$ min) showed MICs against *B. subtilis* in the range of 25 to 50 μM, and the low activity of Ac-WFW underlined the activity-reducing role of high-chain flexibility. The activity spectra of the peptides toward Gram-positive and Gram-negative bacteria were comparable, but changes in the MIC against *E. coli* were more pronounced (Table 1). The MICs of c-WFW (3.1 μM) and the linear Ac-WFW (400 μM) differ by a factor of >130. Increasing the ring size in c-(b3-hW)F(b3-hW) (MIC = 50 μM) raised the MIC 16-fold. The least hydrophobic analogs, c-(Dht)F(Dht) and c-(Igl)F(Igl), also were much less active against *E. coli* than *B. subtilis.* Interestingly, the most hydrophobic peptide, c-(Bal)F(Bal), as well as c-(5MeoW)F(5MeoW), were less active than c-WFW against *E. coli*. Rather than a correlation between activity and retention behavior in RP-HPLC, a threshold value for the t_R seems to exist that separates highly and less active peptides (Table 1; also see Fig. S4 in the supplemental material).

Significant hemolytic activity was revealed only by the most hydrophobic analogs, c-(Bal)F(Bal) and c-(1MeW)F(1-MeW), which caused 70 and 27% hemoglobin release, respectively, from human RBCs at a 200 μM peptide concentration (Table 1).

Permeabilization of outer and inner membranes of *E. coli* (strain ML-35p). The effect of the antimicrobially active cyclic peptides on the outer and inner membrane of *E. coli* is presented in Fig. 4. c-(5fW)F(5fW) and c-(1MeW)F(1MeW) permeabilized the outer membrane of *E. coli* (strain ML-35p) more rapidly than c-(5MeoW)F(5MeoW) and the parent peptide (c-WFW), and the kinetics of permeabilization by b3-hW- and Bal-containing peptides was slow (Fig. 4A). The permeabilization rate ($\Delta OD/\Delta t$) of the investigated peptides (except b3-hW) correlated with their antimicrobial potency against *E. coli* (see Fig. S5 in the supplemental material). Surprisingly, none of the peptides permeabilized the inner membrane appreciably, even at concentrations much higher than the MIC (Fig. 4B). These results point to a major role of LPS in mediating peptide transport across the bacterial outer membrane and a mode of action that does not depend on inner membrane permeabilization.

Peptide binding to POPC and POPC-POPG SUVs. To study peptide binding to lipid bilayers, we chose POPC SUVs to mimic the properties of a eukaryotic cell membrane. POPC-POPG (3:1 [mol/mol]) often is used to mimic the charge properties of cytoplasmic membranes of bacteria (36), although these are composed mainly of zwitterionic 1-palmitoyl-2-oleoyl-*sn*-glycero-3-phosphatidylamine (POPE) and negatively charged POPG (20).

Binding isotherms derived from typical ITC traces (raw data are not shown), given as the molar ratio of bound peptide to accessible lipid (R_b) as a function of the free peptide concentration ($c_{P,f}$), are displayed in Fig. S1 in the supplemental material. Low R_b values for POPC followed the order Ac-WFW ≈ c-(Igl)F(Igl) ≈ c-(Dht)F(Dht) < c-(5MeoW)F(5MeoW) ≈ c-(b3-hW)F(b3-hW) < c-WFW ≈ c-(1MeW)F(1MeW) < c(5fW)F(5fW) ≈ c-(5MeW)F(5MeW) < c-(Bal)F(Bal) (Table 2). A negative bilayer charge enhanced peptide binding. However, after correcting for electrostatic attraction (30, 31, 43), the Gibbs free energies of membrane partitioning ($\Delta G°$) into POPC and POPC-POPG bilayers were comparable

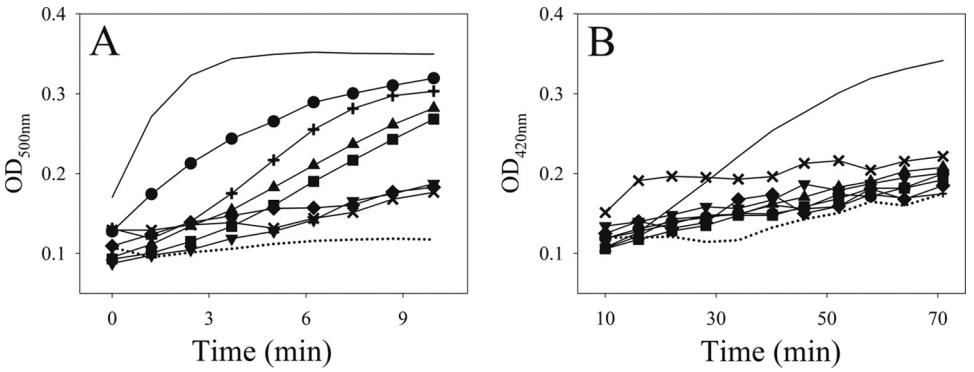

FIG. 4. Outer (A) and inner (B) membrane permeabilization of *E. coli* (strain ML-35p) induced by the cyclic peptides. The peptide concentrations used for outer and inner membrane permeabilization assays were 18 and 162 mM, respectively. The peptides are represented are c-WFW (▲), c-(5MeoW)F(5MeoW) (■), c-(5fW)F(5fW) (●), c-(b3-hW)F(b3-hW) (▼), c-(5MeW)F(5MeW) (◆), c-(1MeW)F(1MeW) (+), and c-(Bal)F(Bal) (×). The wells with PMXB (solid line) and with no peptides (dotted line) were used as controls.

(Table 2; also see Fig. S2 in the supplemental material). The low $\Delta G°$ values for Ac-WFW or c-(b3-hW)F(b3-hW) and c-(Igl)F(Igl) or c-(Dht)F(Dht) emphasize the role of conformational constraints and hydrophobicity of the cyclic peptide in membrane binding. There was a good linear correlation between the partition coefficient, K_0, and the t_R of the cyclic peptides if c-(Dht)F(Dht) is excluded (Fig. S6a in the supplemental material). The observations underline the crucial role of electrostatic interactions in peptide accumulation at the lipid bilayer and demonstrate that nonelectrostatic interactions provide comparable contributions to partitioning into zwitterionic and anionic lipid bilayers.

The contributions of enthalpy ($\Delta H°$) and entropy ($-T\Delta S°$) were highly variable (Table 2; also see Fig. S2 in the supplemental material), and the correlation with t_R was found to be rather poor. Interestingly, $\Delta H°$ and $-T\Delta S°$ are comparable for the lipid binding of c-(Dht)F(Dht), c-(Igl)F(Igl), and the most hydrophobic c-(Bal)F(Bal). The common feature of Dht, Igl, and Bal residues is a reduced dipole moment compared to that of W; however, unlike Igl and Bal, Dht is as amphipathic as W. The binding of the other peptides, including the linear Ac-WFW, to both POPC and POPC-POPG systems is driven by enthalpy (Table 2; also see Fig. S2 in the supplemental material). The pronounced $\Delta H°$ of c-(5MeoW)F(5MeoW) and c-(5fW)F(5fW) correlates with a slightly increased peptide hydrophobicity (Table 1) and an enhanced hydrogen-bonding tendency compared to that of the cyclic parent peptide. The high enthalpy contribution is associated with low negative values of $-T\Delta S°$ (Table 2; also see Fig. S2 in the supplemental material). The $\Delta H°$ of c-(b3-hW)F(b3-hW), c-(5MeW)F(5MeW), and c-(1MeW)F(1MeW) binding ranges between ~−20 and −27 kJ/mol. The common feature of theses peptides is a mean hydrophobicity reflected by a t_R of ~20 min (Table 1). Except for the Dht-, Igl-, and Bal-containing cyclic peptides, peptide binding to POPC and POPC-POPG lipid bilayers is in good agreement with the nonclassical hydrophobic effect described for other CAPs (3, 47, 51). A comparable behavior has been reported for two W-containing gramicidin S analogs interacting with POPC (28).

Binding to POPC-LA, POPC–r-LPS, and POPC–s-LPS (12:1 [mol/mol]) SUVs. To investigate the role of LPS in peptide activity against *E. coli*, we studied peptide binding to LA, r-LPS (Rd mutant), and s-LPS incorporated into POPC bilayers at a molar ratio of 1:12. The binding isotherms are presented in Fig. S1 in the supplemental material, and the derived thermodynamic parameters are summarized in Table 3. The K_0 values for POPC–s-LPS bilayers were almost 1 order of magnitude higher than those for bilayers doped with O-antigen-deficient r-LPS or LA. The affinity of Ac-WFW to LA-, r-LPS-, or s-LPS-containing liposomes was low. The affinity of the

TABLE 2. Thermodynamic parameters for peptide binding to POPC and POPC-POPG (3:1 [mol/mol]) SUVs

Peptide denotation	POPC					POPC-POPG (3:1 [mol/mol])				
	R_b[a] (mol/mol)	$\Delta H°$ (kJ/mol)	$-T\Delta S°$ (kJ/mol)	$\Delta G°$ (kJ/mol)	K_0 (M^{-1})	R_b[a] (mol/mol)	$\Delta H°$ (kJ/mol)	$-T\Delta S°$ (kJ/mol)	$\Delta G°$ (kJ/mol)	K_0 (M^{-1})
c-(Dht)F(Dht)	1.4×10^{-2}	−12.1	−14.5	−26.6	5.4×10^2	1.2×10^{-1}	−11.4	−19.0	−30.4	2.4×10^3
c-(Igl)F(Igl)	0.8×10^{-2}	−13.0	−11.9	−24.9	2.8×10^2	0.8×10^{-1}	−20.0	−7.8	−27.8	8.9×10^2
c-WFW	7.2×10^{-2}	−31.2	−1.8	−33.0	6.7×10^3	2.2×10^{-1}	−23.5	−11.0	−34.5	1.2×10^4
c-(5MeoW)F(5MeoW)	5.0×10^{-2}	−40.0	8.2	−31.8	4.1×10^3	1.4×10^{-1}	−37.6	4.3	−33.3	7.5×10^3
c-(5fW)F(5fW)	9.3×10^{-2}	−40.7	6.0	−34.7	1.3×10^4	1.7×10^{-1}	−41.6	6.2	−35.4	1.7×10^4
c-(b3-hW)F(b3-hW)	4.6×10^{-2}	−19.8	−10.7	−30.5	2.5×10^3	1.6×10^{-1}	−23.3	−8.2	−31.5	3.7×10^3
c-(5MeW)F(5MeW)	9.6×10^{-2}	−21.8	−12.2	−34.0	9.9×10^3	2.0×10^{-1}	−25.9	−9.0	−34.9	1.4×10^4
c-(1MeW)F(1MeW)	7.6×10^{-2}	−27.6	−7.2	−34.8	1.3×10^4	1.9×10^{-1}	−27.7	−6.1	−33.8	9.0×10^3
c-(Bal)F(Bal)	11.2×10^{-2}	−18.9	−15.2	−34.1	1.0×10^4	3.0×10^{-1}	−16.4	−17.2	−33.6	8.4×10^3
Ac-WFW	1.0×10^{-2}	−30.0	4.0	−26.0	4.4×10^2	0.9×10^{-1}	−28.4	−0.2	−28.6	1.2×10^3

[a] These values were taken at $c_{P,f} = 30$ μM.

TABLE 3. Thermodynamic parameters for peptide binding to POPC-LA (12:1 [mol/mol]), POPC–r-LPS (12:1 [mol/mol]), and POPC–s-LPS (12:1 [mol/mol]) SUVs

Peptide denotation	POPC-LA (12:1 [mol/mol])				POPC–r-LPS (12:1 [mol/mol])				POPC–s-LPS (12:1 [mol/mol])			
	R_b[a] (mol/mol)	ΔH° (kJ/mol)	$-T\Delta S^\circ$ (kJ/mol)	ΔG° (kJ/mol)	K_0 (M^{-1})	R_b[a] (mol/mol)	ΔH° (kJ/mol)	$-T\Delta S^\circ$ (kJ/mol)	ΔG° (kJ/mol)	K_0 (M^{-1})	R_b[a] (mol/mol)	ΔH° (kJ/mol)	$-T\Delta S^\circ$ (kJ/mol)	ΔG° (kJ/mol)	K_0 (M^{-1})
c-(Dht)F(Dht)	1.1×10^{-1}	−10.0	−19.4	−29.4	1.6×10^3	4.0×10^{-1}	−4.1	−30.2	−34.3	1.1×10^4	4.7×10^{-1}	−7.7	−28.9	−36.6	2.7×10^4
c-(Igl)F(Igl)	0.7×10^{-1}	−9.30	−18.0	−27.3	7.3×10^2	1.2×10^{-1}	−11.2	−20.4	−31.6	3.8×10^3	3.6×10^{-1}	−15.0	−20.4	−35.4	1.7×10^4
c-WFW	1.4×10^{-1}	−27.1	−4.7	−31.8	4.2×10^3	2.6×10^{-1}	−19.5	−14.5	−34.0	9.9×10^3	5.2×10^{-1}	−28.7	−7.0	−35.7	1.9×10^4
c-(5MeoW)F(5MeoW)	0.9×10^{-1}	−40.4	10.8	−29.6	1.8×10^3	1.7×10^{-1}	−30.0	−0.8	−30.8	2.8×10^3	3.8×10^{-1}	−36.0	0.3	−35.7	1.9×10^4
c-(5fW)F(5fW)	1.6×10^{-1}	−33.7	−1.1	−34.8	1.3×10^4	2.5×10^{-1}	−26.7	−7.0	−33.7	8.7×10^3	6.0×10^{-1}	−28.0	−10.6	−38.6	5.8×10^4
c-(b3-hW)F(b3-hW)	1.3×10^{-1}	−18.3	−12.2	−30.5	2.5×10^3	2.3×10^{-1}	−17.6	−13.8	−31.4	3.5×10^3	4.8×10^{-1}	−20.5	−14.3	−34.8	1.3×10^4
c-(5MeW)F(5MeW)	1.7×10^{-1}	−20.2	−12.0	−32.2	4.8×10^3	2.2×10^{-1}	−25.0	−6.0	−31.0	3.0×10^3	4.6×10^{-1}	−30.0	−4.5	−34.5	1.2×10^4
c-(1MeW)F(1MeW)	1.5×10^{-1}	−22.6	−11.2	−33.8	9.1×10^3	2.3×10^{-1}	−23.5	−9.7	−33.2	7.0×10^3	4.9×10^{-1}	−30.7	−5.2	−35.9	2.0×10^4
c-(Bal)F(Bal)	2.4×10^{-1}	−15.4	−18.3	−33.7	8.7×10^3	2.6×10^{-1}	−22.9	−9.3	−32.2	4.8×10^3	6.2×10^{-1}	−28.4	−6.7	−35.1	1.5×10^4
Ac-WFW	0.5×10^{-1}	−29.4	5.3	−24.1	2.1×10^2	0.5×10^{-1}	−30.0	3.0	−27.0	6.5×10^2	1.9×10^{-1}	−33.3	2.3	−31.0	3.0×10^3

[a] These values were taken at $c_{P,f} = 30$ μM.

cyclic sequences [except c-(Dht)F(Dht)] to the LA-containing liposomes was comparable to binding to POPC-POPG bilayers and correlated with peptide hydrophobicity. The correlation was lost for the r-LPS system, and binding to s-LPS-containing liposomes was independent of the peptide properties [except for c-(5fW)F(5fW)] (Table 3; also see Fig. S3 and S6 in the supplemental material).

The partitioning of the hydrophilic c-(Dht)F(Dht) and c-(Igl)F(Igl) peptides into LPS-doped lipid vesicles was driven by entropy (Table 3; also see Fig. S3 in the supplemental material), whereas the binding of the other cyclic peptides as well as Ac-WFW to liposomes containing LA and the two LPS mutants was dominated by enthalpy changes (Table 3; also see Fig. S3 in the supplemental material).

To investigate whether the enhanced partitioning of the cyclic peptides into LPS-doped POPC bilayers is due to electrostatic interactions, titrations of c-WFW with POPC–r-LPS (12:1 [mol/mol]) and POPC–s-LPS (12:1 [mol/mol]) were performed at different NaF concentrations. Binding was strongest to bilayers containing O-antigen-presenting s-LPS, and partitioning only slightly depended on the ionic strength (Fig. 5). c-WFW partitioning into POPC–r-LPS was almost independent of the ionic strength. As both r-LPS and s-LPS bear the same charge (Fig. 2), these results underline the significant role of the O antigen in peptide partitioning into LPS-rich bilayers.

DISCUSSION

The introduction of conformational constraints in small RW-rich peptides by cyclization has been found to enhance the antimicrobial activity, in particular against Gram-negative *E. coli* (14, 50). R- and W-rich clusters seem to be responsible for the selectivity increase as well as for the high affinity to lipid bilayers (14), and LPS moieties have been suggested to exert a strong activity-modulating effect (29). The replacement of W residues in c-WFW with various unnatural amino acids, such as Dht, Igl, 5MeoW, 5fW, b3-hW, 5MeW, 1MeW, and Bal (Fig. 1), made possible a systematic investigation of the importance of the aromatic cluster for peptide interactions with artificial lipid systems and with the outer and inner membranes of *E. coli* and for the biological activity spectrum.

Structure-activity relationships. Membrane activity of CAPs depends on both electrostatic accumulation near negatively charged membrane constituents and insertion into the lipid matrix, which finally results in a breakdown of the barrier function of the membrane by many peptides (15). This idea is supported by the correlation of peptide binding to neutral and negatively charged lipid bilayers with hemolytic and antibacterial activities (Tables 1 and 2). Low peptide concentrations in the vicinity of neutral lipid bilayers are responsible for low hemolytic activity, whereas electrostatic attraction favors binding to POPC-POPG bilayers (16, 20). However, the binding and partitioning of the cyclic peptides was not sufficient to induce the permeabilization of the cytoplasmic membrane of *E. coli* at the MIC.

Peptide activity against biological systems is well reflected in the sequence-dependent profile of binding to phospholipid bilayers. The partitioning of the cyclic peptides is much stronger than that of the linear analog. The significant role of

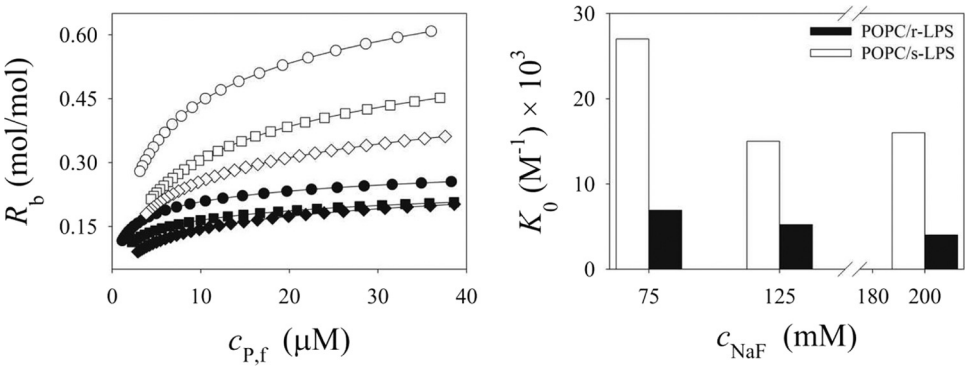

FIG. 5. Binding isotherms and partition coefficient values for c-WFW binding to r-LPS- and s-LPS-bearing POPC SUVs at different ionic strengths. The salt concentrations (c_{NaF}) were 75 mM (●), 125 mM (■), and 200 mM (◆) for POPC–r-LPS (12:1 [mol/mol]), and they were 75 mM (○), 125 mM (□), and 200 mM (◇) for POPC–s-LPS (12:1 [mol/mol]) lipid bilayers in 10 mM phosphate buffer, pH 7.4. The fit parameters are listed in Table S5 in the supplemental material.

hydrophobicity and the amphipathic nature of the W residues was supported by the distinct reduction in the antimicrobial effect and lipid bilayer binding of c-(Dht)F(Dht) and c-(Igl)F(Igl) (Tables 1 and 2). The small enthalpic contribution to bilayer binding for Dht-containing peptides is compensated for by a more favorable entropic term (Table 2), which is in agreement with the classical hydrophobic effect (44). This effect was observed for the antimicrobial peptide dicynthaurin as well (49). The authors considered water and counterion release from the peptide and a sodium binding equilibrium at the lipid headgroups as the major driving forces for peptide-membrane interactions. The incorporation of a nonamphipathic but highly hydrophobic residue (i.e., Bal) reduced only the anti-*E. coli* activity but not bilayer binding (Tables 1 and 2). This is in contrast with the results on the bactericidal activity of a 15-residue Bal-modified lactoferricin derivative, which exhibited higher antimicrobial activity than the parent peptide (46).

Whereas the preferential location of the W residue at the membrane interface has been attributed to its dipole and quadrupole moments and its ability to form hydrogen bonds with both water and polar lipid headgroup moieties (1, 33, 41), these physicochemical properties did not make any distinguished contribution to the bilayer binding of our cyclic hexapeptides, as reflected by c-(1MeW)F(1MeW), c-(5fW)F(5fW), and c-(5MeoW)F(5MeoW) (Table 2). Because of the higher quadrupole moment of the indole ring in c-(5MeoW)F(5MeoW) compared to that of c-(5fW)F(5fW) (42), we expected a higher bilayer affinity of the former peptide (1, 33). However, the opposite was observed (Table 2). This underlines the contribution of other driving forces, such as the dominating role of hydrophobicity, for the insertion of the WFW cluster into a phospholipid membrane.

The introduction of the β-amino acid b3-hW in c-WFW might disturb the β-turn motifs in c-WFW (6) and induce a different amphipathic conformation. A pronounced conformational change was shown by CD spectroscopy (Fig. 3). Recent studies with analogs of gramicidin S with ring sizes ranging from 10 to 16 amino acid residues confirm the importance of amphipathicity induced by the β-turn/β-sheet structure in interaction with membranes (27). The disruption of the structure by increasing the size of the cyclic peptide weakened the peptides' interaction with POPC vesicles and reduced their hemolytic, antimicrobial, and antifungal activities. Because the t_R value of c-(b3-hW)F(b3-hW) was higher than that of c-WFW (Table 1), other parameters than global peptide hydrophobicity and amphipathicity must be responsible for reduced bilayer partitioning and antimicrobial activities, especially against *E. coli*.

Peptide binding to liposomes composed of LA, r-LPS, and s-LPS. Peptide transport across the outer wall of Gram-negative bacteria is a prerequisite for interaction with the inner membrane or transport to intracellular targets. LPS, the major component of the outer membrane, might act as a protective shield, as suggested for lactoferricin-derived peptides (21). It may serve as a trap for polycationic substances and thus inhibit the transport of antibiotic agents (2). On the other hand, CAPs may increase outer membrane permeability by disordering the LPS layer. A mechanism of self-promoted uptake has been suggested to facilitate translocation and improve peptide accessibility to the inner membrane (23).

Our results demonstrate that the permeabilization of the outer membrane of *E. coli* induced by the active cyclic peptides [except c-(5fW)F(5fW)] correlates well with the antimicrobial activity (Table 1; also see Fig. S5 in the supplemental material). We also found that peptide binding and partitioning are highest to lipid bilayers doped with wild-type LPS (Table 3). This correlates with maximal antimicrobial activity of c-WFW against native *E. coli* strains and a reduced effect on O-antigen- and outer core-deficient LPS mutant strains (29). The observations confirm the activity-modulating role of the outer *E. coli* wall and the particular function of O-antigen polysaccharides for the activity of our cyclic hexapeptides.

A prominent role of W and R residues and conformational constraints in LPS binding is supported by the high affinity of the cyclic β-sheet CAP tachyplesin I for LPS compared to that of acidic phospholipids, whereas a linear analog and a helical magainin peptide could not discriminate between the two acidic lipids (25). The LA moiety is supposed to represent the recognition site, and the cyclic structure is crucial for specific binding. The affinities of our hexapeptides to POPC-LA and POPC-POPG bilayers with identical negative surface charge densities were comparable with respect to the magnitude and

sequence dependency of the thermodynamic parameters (Tables 1 and 2; also see Fig. S1 in the supplemental material). On the basis of this observation, we conclude that hydrophobic peptide-LPS interactions are essential for efficient transport across the bacterial outer membrane but that LA does not act as a specific activity-modulating binding site for the hexapeptides. This is in accordance with observations on lactoferricin peptides, suggesting that the tightly packed fatty acid in LA is not the primary site of interaction (21).

Further studies with lactoferricin-derived peptides and LPS mutant *E. coli* strains also underlined the importance of the appropriate locations of R and W residues for antimicrobial activity. It has been suggested that the peptides first interact with the negative charges present in the inner core of LPS, leading to the disorganization of the outer membrane and facilitating the approach of W residues to LA to promote hydrophobic interactions (19). In contrast, Farnaud et al. (21) suggested that ionic interactions between lactoferricin peptides and LPS are strong in the absence of the O-antigen region because of the unmasking of the negatively charged phosphate groups in the inner core. r-LPS contains roughly nine negatively charged phosphate groups per molecule, thus peptide binding was expected to be stronger than that to bilayers mixed with LA, which bears two $[-OPO_3]^{-2}$ groups per molecule. We found that the increase in negative charge in r-LPS-doped bilayers compared to that of the POPC-LA system only slightly enhanced binding, except for the most hydrophilic peptides (Dht- and Igl-containing cyclic peptides) (Table 3). Furthermore, the low salt dependency of c-WFW binding to POPC–r-LPS bilayers (Fig. 5) confirms a minor role of the direct electrostatic interaction of the peptide with LPS inner core charges.

In s-LPS-doped bilayers, however, partitioning distinctly increased compared to that for r-LPS. In contrast to our expectation based on the differentiated activity pattern against *E. coli*, sequence-related differences in the free energy of binding disappeared in the presence of O-antigen oligosaccharides, with the exception of c-(5fW)F(5fW) (Table 3; also see Fig. S3A in the supplemental material). The fact that the partitioning pattern of the cyclic peptides revealed little variation points to a dominating influence of electrostatic interactions upon binding. As the result of enhanced accumulation, peptide partitioning might increase. This is surprising, as both r-LPS and s-LPS have the same distribution of negatively charged phosphate groups. Moreover, favorable contributions of the sugar moieties to peptide binding to s-LPS might also be considered. Carbohydrates interact in a favorable manner with peptides and proteins via stacking involving aromatic side chains (34). The π-electron distribution, surface area, and flexibility of the aromatic systems affect the magnitude of the interaction. In recent studies of a β-hairpin peptide containing a W residue as well as a glucosyl or galactosyl analog of serine, strong intramolecular carbohydrate–π-electron interactions (2.1 to 3.3 kJ/mol; stronger than π-π or cation-π interactions) were found to stabilize the peptide's secondary structure (34).

The reason why distinct differences in the hydrogen-bonding ability, dipole moment, and aromaticity of the cyclic peptides are not reflected in the thermodynamic characteristics of their interactions with LPS-containing lipid bilayers remains to be elucidated.

Conclusions. In this study, we showed that peptide activity against bacteria and RBCs can be explained on the basis of peptide accessibility to the lipid matrices of the target membranes. Accumulation is driven by electrostatic interactions, and membrane partitioning is determined by hydrophobic interactions. Peptide hydrophobicity and backbone constraints are the crucial determinants of biological activity. Low peptide hydrophobicity and the conformational flexibility of the peptides reduced binding, thus confirming the suggestion that peptide interactions with the cytoplasmic membrane determine the biological effect. Other modifications in the hydrophobic cluster of the cyclic hexapeptides, such as hydrogen-bonding ability and the dipole and quadrupole moments, have a minor influence upon peptide interaction with biological systems and model membranes.

Differences in the negative surface charge and the content of phosphatidylethanolamine of the plasma membranes might be one reason for the different susceptibilities of *E. coli* and *B. subtilis*. However, interactions with the outer membrane LPSs influence peptide transport across the wall and determine the activity profile of the peptides against *E. coli*. While interactions with the LA domain are not particularly strong, peptide partitioning is favored in POPC–r-LPS and even more pronounced in the presence of s-LPS. The O-antigen of LPS is essential for avid partitioning and likely decisive for efficient peptide transport across the outer *E. coli* wall. Although properties of the aromatic motif had a minor influence on the free energy of partitioning in the s-LPS-doped bilayer, high variability was found in the contribution of enthalpy and entropy. Specific peptide interactions between the structural variants of W and LPS moieties providing an explanation for the differentiated outer membrane permeability and activity profile of the peptide against *E. coli* could not be identified. Furthermore, the fact that none of the peptides displayed a pronounced capacity to permeabilize the cytoplasmic membrane (even at concentrations above the MICs) suggests that the bactericidal activity of the cyclic peptides against *E. coli* is not primarily a consequence of inner-membrane disruption. Most likely other mechanisms are involved, such as the phase separation of lipids (8) or processes that allow the passage of molecules smaller than ONPG through the cytoplasmic membrane.

ACKNOWLEDGMENTS

We gratefully acknowledge technical support by Bernhard Schmikale, Annerose Klose, Heike Nikolenko, Nadin Jahnke, and Gerdi Kemmer (all at FMP).

We thank Michael Bienert and Michael Beyermann (both at FMP) for fruitful discussions.

REFERENCES

1. **Aliste, M. P., J. L. MacCallum, and D. P. Tieleman.** 2003. Molecular dynamics simulations of pentapeptides at interfaces: salt bridge and cation–π interactions. Biochemistry **42:**8976–8987.
2. **Andrä, J., M. H. J. Koch, R. Bartels, and K. Brandenburg.** 2004. Biophysical characterization of endotoxin inactivation by NK-2, an antimicrobial peptide derived from mammalian NK-lysin. Antimicrob. Agents Chemother. **48:** 1593–1599.
3. **Andrushchenko, V. V., M. H. Aarabi, L. T. Nguyen, E. J. Prenner, and H. J. Vogel.** 2008. Thermodynamics of the interactions of tryptophan-rich cathelicidin antimicrobial peptides with model and natural membranes. Biochim. Biophys. Acta **1778:**1004–1014.
4. **Appelt, C., A. K. Schrey, J. A. Söderhäll, and P. Schmieder.** 2007. Design of antimicrobial compounds based on peptide structures. Bioorg. Med. Chem. Lett. **17:**2334–2337.

5. **Appelt, C., A. Wessolowski, J. A. Söderhäll, M. Dathe, and P. Schmieder.** 2005. Structure of the antimicrobial, cationic hexapeptide cyclo(RRWWRF) and its analogues in solution and bound to detergent micelles. Chem. BioChem. **6:**1654–1662.
6. **Appelt, C., A. Wessolowski, M. Dathe, and P. Schmieder.** 2008. Structures of cyclic, antimicrobial peptides in a membrane-mimicking environment define requirements for activity. J. Pept. Sci. **14:**524–527.
7. **Appelt, C., F. Eisenmenger, R. Kühne, P. Schmieder, and J. A. Söderhäll.** 2005. Interaction of the antimicrobial peptide cyclo(RRWWRF) with membranes by molecular dynamics simulations. Biophys. J. **89:**2296–2306.
8. **Arouri, A., M. Dathe, and A. Blume.** 2009. Peptide induced demixing in PG/PE lipid mixtures: a mechanism for the specificity of antimicrobial peptides towards bacterial membranes? Biochim. Biophys. Acta **1788:**650–659.
9. **Bagheri, M.** 2010. Synthesis and thermodynamic characterization of small cyclic antimicrobial arginine and tryptophan-rich peptides with selectivity for Gram-negative bacteria, p. 87–109. *In* A. Giuliani and A. C. Rinaldi (ed.), Antimicrobial peptides: methods and protocols, methods in molecular biology. Humana Press, New York, NY.
10. **Bagheri, M., M. Beyermann, and M. Dathe.** 2009. Immobilization reduces the activity of surface-bound cationic antimicrobial peptides with no influence upon the activity spectrum. Antimicrob. Agents Chemother. **53:**1132–1141.
11. **Bennett-Guerrero, E., et al.** 2000. Preparation and preclinical evaluation of a novel liposomal complete-core lipopolysaccharide Vaccine. Infect. Immun. **68:**6202–6208.
12. **Blondelle, S. E., and R. A. Houghten.** 1996. Novel antimicrobial compounds identified using synthetic combinatorial library technology. Trends Biotechnol. **14:**60–65.
13. **Brandenburg, K., M. D. Arraiza, G. Lehwark-Ivetot, I. Moriyon, and U. Zähringer.** 2002. The interaction of rough and smooth form lipopolysaccharides with polymyxins as studied by titration calorimetry. Thermochim. Acta **394:**53–61.
14. **Dathe, M., H. Nikolenko, J. Klose, and M. Bienert.** 2004. Cyclization increases the antimicrobial activity and selectivity of arginine- and tryptophan-containing hexapeptides. Biochemistry **43:**9140–9150.
15. **Dathe, M., et al.** 2002. General aspects of peptide selectivity towards lipid bilayers and cell membranes studied by variation of the structural parameters of amphipathic helical model peptides. Biochim. Biophys. Acta **1558:**171–186.
16. **Dathe, M., and T. Wieprecht.** 1999. Structural features of helical antimicrobial peptides: their potential to modulate activity on model membranes and biological cells. Biochim. Biophys. Acta **1462:**71–87.
17. **Deber, C. M., L.-P. Liu, C. Wang, N. K. Goto, and R. A. F. Reithmeier.** 2002. The hydrophobicity threshold for peptide insertion into membranes, p. 465–479. *In* S. A. Simon and T. J. McIntosh (ed.), Current topics in membranes, peptide-lipid interactions. Academic Press, Elsevier Science, San Diego, CA.
18. **Dijkstra, J., J. L. Ryan, and F. C. Szoka.** 1988. A procedure for the efficient incorporation of wild-type lipopolysaccharide into liposomes for use in immunological studies. J. Immunol. Methods **114:**197–205.
19. **Elass-Rochard, E., et al.** 1995. Lactoferrin-lipopolysaccharide interaction: involvement of the 28-34 loop region of human lactoferrin in the high-affinity binding to *Escherichia coli* 055B5 lipopolysaccharide. Biochem. J. **312:**839–845.
20. **Epand, R. M., and R. F. Epand.** 2009. Domains in bacterial membranes and the action of antimicrobial agents. Mol. Biosyst. **5:**580–587.
21. **Farnaud, S., et al.** 2004. Interactions of lactoferricin-derived peptides with LPS and antimicrobial activity. FEMS Microbiol. Lett. **233:**193–199.
22. **Gennaro, R., and M. Zanetti.** 2000. Structural features and biological activities of the cathelicidin-derived antimicrobial peptides. Biopolymers **55:**31–49.
23. **Hancock, R. E. W., and D. S. Chapple.** 1999. Peptide antibiotics. Antimicrob. Agents Chemother. **43:**1317–1323.
24. **Hilpert, K., R. Volkmer-Engert, T. Walter, and R. E. W. Hancock.** 2005. High-throughput generation of small antibacterial peptides with improved activity. Nat. Biotechnol. **23:**1008–1012.
25. **Hirakura, Y., S. Kobayashi, and K. Matsuzaki.** 2002. Specific interactions of the antimicrobial peptide cyclic beta-sheet tachyplesin I with lipopolysaccharides. Biochim. Biophys. Acta **1562:**32–36.
26. **Jelokhani-Niaraki, M., E. J. Prenner, C. M. Kay, R. N. McElhaney, and R. S. Hodges.** 2002. Conformation and interaction of the cyclic cationic antimicrobial peptides in lipid bilayers. J. Pept. Res. **60:**23–36.
27. **Jelokhani-Niaraki, M., L. H. Kondejewski, L. C. Wheaton, and R. S. Hodges.** 2009. Effect of ring size on conformation and biological activity of cyclic cationic antimicrobial peptides. J. Med. Chem. **52:**2090–2097.
28. **Jelokhani-Niaraki, M., R. S. Hodges, J. E. Meissner, U. E. Hassenstein, and L. Wheaton.** 2008. Interaction of gramicidin S and its aromatic amino-acid analog with phospholipid membranes. Biophys. J. **95:**3306–3321.
29. **Junkes, C., et al.** 2008. The interaction of arginine- and tryptophan-rich cyclic hexapeptides with Escherichia coli membranes. J. Pept. Sci. **14:**535–543.
30. **Keller, S., H. Heerklotz, and A. Blume.** 2006. Monitoring lipid membrane translocation of sodium dodecyl sulfate by isothermal titration calorimetry. J. Am. Chem. Soc. **128:**1279–1286.
31. **Keller, S., M. Böthe, M. Bienert, M. Dathe, and A. Blume.** 2007. A simple fluorescence-spectroscopic membrane translocation assay. Chem. BioChem. **8:**546–552.
32. **Kemmer, G., and S. Keller.** 2010. Nonlinear least-squares data fitting in Excel spreadsheets. Nat. Protoc. **5:**267–281.
33. **Khandelia, H., and Y. N. Kaznessis.** 2007. Cation-π interactions stabilize the structure of the antimicrobial peptide indolicidin near membranes: molecular dynamics simulations. J. Phys. Chem. B. **111:**242–250.
34. **Laughrey, Z. R., S. E. Kiehna, A. J. Riemen, and M. L. Waters.** 2008. Carbohydrate-π interactions: what are they worth? J. Am. Chem. Soc. **130:**14625–14633.
35. **Lehrer, R. I., A. Barton, and T. Ganz.** 1988. Concurrent assessment of inner and outer membrane permeabilization and bacteriolysis in *E. coli* by multiple-wavelength spectrophotometry. J. Immunol. Methods **108:**153–158.
36. **Lohner, K., and F. Prossnigg.** 2009. Biological activity and structural aspects of PGLa interaction with membrane mimetic systems. Biochim. Biophys. Acta **1788:**1656–1666.
37. **McClellan, A. L.** 1963. Tables of experimental dipole moments, p. 280-325. W. H. Freeman and Company, San Francisco, CA.
38. **McIntire, F. C., H. W. Sievert, G. H. Barlow, R. A. Finley, and A. Y. Lee.** 1967. Chemical, physical, and biological properties of a lipopolysaccharide from *Escherichia coli* K-235. Biochemistry **6:**2363–2372.
39. **Pritz, S., M. Pätzel, G. Szeimies, M. Dathe, and M. Bienert.** 2007. Synthesis of a chiral amino acid with bicyclo[1.1.1]pentane moiety and its incorporation into linear and cyclic antimicrobial peptides. Org. Biomol. Chem. **5:**1789–1794.
40. **Raetz, C. R. H., and C. Whitfield.** 2002. Lipopolysaccharide endotoxins. Annu. Rev. Biochem. **71:**635–700.
41. **Schibli, D. J., R. F. Epand, H. J. Vogel, and R. M. Epand.** 2002. Tryptophan-rich antimicrobial peptides: comparative properties and membrane interactions. Biochem. Cell Biol. **80:**667–677.
42. **Schweizer, S., and J. Reed.** 2008. Effect of variation of the strength of the aromatic interactions of tryptophan on the cooperative structural refolding behavior of a peptide from HIV 1. Biophys. J. **95:**3381–3390.
43. **Seelig, J.** 1997. Titration calorimetry of lipid-peptide interactions. Biochim. Biophys. Acta **1331:**103–116.
44. **Seelig, J., and P. Ganz.** 1991. Nonclassical hydrophobic effect in membrane binding equilibria. Biochemistry **30:**9354–9359.
45. **Strøm, M. B., et al.** 2003. The pharmacophore of short cationic antibacterial peptides. J. Med. Chem. **46:**1567–1570.
46. **Strøm, M. B., et al.** 2002. Important structural features of 15-residue lactoferricin derivatives and methods for improvement of antimicrobial activity. Biochem. Cell Biol. **80:**65–74.
47. **Svenson, J., B.-O. Brandsdal, W. Stensen, and J. S. Svendsen.** 2007. Albumin binding of short cationic antimicrobial micropeptides and its influence on the *in vitro* bactericidal effect. J. Med. Chem. **50:**3334–3339.
48. **Tsamaloukas, A. D., S. Keller, and H. Heerklotz.** 2007. Uptake and release protocol for assessing membrane binding and permeation by way of isothermal titration calorimetry. Nat. Protoc. **2:**695–704.
49. **Wen, S., M. Majerowicz, A. Waring, and F. Bringezu.** 2007. Dicynthaurin (ala) monomer interaction with phospholipid bilayers studied by fluorescence leakage and isothermal titration calorimetry. J. Phys. Chem. B. **111:**6280–6287.
50. **Wessolowski, A., M. Bienert, and M. Dathe.** 2004. Antimicrobial activity of arginine- and tryptophan-rich hexapeptides: the effects of aromatic clusters, D-amino acid substitution and cyclization. J. Pept. Res. **64:**159–169.
51. **Wieprecht, T., O. Apostolov, M. Beyermann, and J. Seelig.** 2000. Membrane binding and pore formation of the antibacterial peptide PGLa: thermodynamic and mechanistic aspects. Biochemistry **39:**442–452.
52. **Zasloff, M.** 2002. Antimicrobial peptides of multicellular organisms. Nature **415:**389–395.